https://doi.org/10.5194/egusphere-2026-6751
Preprint. Discussion started: 24 November 2026
© Author(s) 2026. CC BY 4.0 License.

Traffic-related enhancement of new particle growth in an urban tunnel

Fuyang Zhang [a], Jinsheng Zhang [b, *], Jiayuan Liu [a], Yajun Wu [e], Zongyan Lv[f], Kexin Liu [a], Bin Sun [a], Qijun Zhang [a], Lin Wu [a], Miao Tang [c], Ning Yang [c, *], Wei Hu [d], Hongjun Mao [a], Jianfei Peng [a, *]

a Tianjin Key Laboratory of Urban Transport Emission Research & State Environmental Protection Key Laboratory of Urban Ambient Air Particulate Matter Pollution Prevention and Control, College of Environmental Science and Engineering, Nankai University, Tianjin 300071, China

b School of Environmental Science and Safety Engineering, Tianjin University of Technology, Tianjin 300384, China

c Tianjin Eco-Environmental Monitoring Center, Tianjin 300191, China.

d Institute of Surface-Earth System Science, Tianjin University, Tianjin 300072, China

e National Engineering Research Center of Urban Environmental Pollution Control, Beijing Municipal Research Institute of Eco-Environmental Protection, Beijing 100037, China

f School of Energy and Power Engineering, Shandong University, Jinan 250061, China

Corresponding authors:

Jianfei Peng (J.F. Peng): pengjianfei@nankai.edu.cn

Jinsheng Zhang (J.S. Zhang): jinshengz@nankai.edu.cn

Ning Yang (N. Yang): 13820388835@163.com

https://doi.org/10.5194/egusphere-2026-6751
Preprint. Discussion started: 24 November 2026
© Author(s) 2026. CC BY 4.0 License.



Abstract

New particle formation (NPF) in urban air often shows rapid nucleation and growth, yet the role of vehicular emissions remains unclear. We conducted a two-week tunnel experiment in Tianjin, China, to investigate traffic-related enhancement of new-particle growth within the measured 10-25 nm range under photochemically suppressed conditions. The particle number concentration (PNC) difference between the tunnel exit and entrance averaged 1.1×10^4 cm^{-3} during non-NPF days and reached 4.6×10^4 cm^{-3} during the selected NPF event days, indicating additional growth into or within the measured range beyond primary emissions. Growth features appeared approximately 1.3 h earlier at the exit, with a higher apparent growth rate than at the entrance (6.4 versus 5.3 nm h^{-1}). After subtracting the primary-emission reference, traffic-related processes accounted for approximately 24.4% of PNC_{10-25} under near-source tunnel conditions, with an incremental growth estimate of 7.0 nm h^{-1} over the 6-min transit. Dynamic VBS modeling predicted effective growth rates of 6.3-13.7 nm h^{-1} across volatility-sensitivity scenarios, encompassing the observed value and supporting the physical plausibility of this near-source growth. These results indicate that vehicle exhaust may release lower-volatility traffic-related condensable vapors that enhance new-particle growth, highlighting their potential importance for particle number concentrations and associated health implications.

Keywords:

new particle formation, growth rates, tunnel experiment, vehicular emissions

https://doi.org/10.5194/egusphere-2026-6751
Preprint. Discussion started: 24 November 2026
© Author(s) 2026. CC BY 4.0 License.

1. Introduction

Atmospheric new particle formation (NPF) refers to the nucleation and subsequent growth of gas-phase molecules into measurable atmospheric particles (Chen et al., 2023; Guo et al., 2020). As a dominant source of particle number concentrations (PNC), NPF directly contributes over 50% of global cloud condensation nuclei, thereby significantly regulating cloud properties and climate dynamics (Guo et al., 2020; Gordon et al., 2017; Zhang et al., 2012; Guo et al., 2014). Beyond climate relevance, the rapid growth of newly formed particles substantially contributes to regional haze pollution, accounting for 30-70% of fine particulate matter ($PM_{2.5}$) in Chinese megacities (Peng et al., 2021; Zhao et al., 2024; Deng et al., 2020; Guo et al., 2014). In particular, vehicle emissions represent an important anthropogenic source of precursor vapors that may contribute to particle formation and growth in urban air. Traffic-related ultrafine particles are also epidemiologically linked to increased respiratory and cardiovascular morbidity and mortality, posing substantial public health burdens (Qi et al., 2022; Lelieveld and Pöschl, 2017; Zheng et al., 2025).

In urban environments, NPF can still occur frequently despite high pre-existing particle loading (Brean et al., 2024; Li et al., 2022; Qiao et al., 2021). Observed nucleation rates in polluted areas exceed those in rural or remote areas by 3 to 5 times, even under strong coagulation sink (CoagS) (Wang et al., 2013; Peng et al., 2014; Hong et al., 2023; Zhou et al., 2021; Kalkavouras et al., 2020), indicating unresolved anthropogenic drivers. Current evidence shows that anthropogenic emissions contribute importantly to urban NPF (Wang et al., 2013; Peng et al., 2014; Hong et al., 2023; Zhou et al., 2021; Kalkavouras et al., 2020; Yao et al., 2018; Shang et al., 2023; Guo et al., 2020; Wang et al., 2020; Brean et al., 2025). In particular, acid and alkaline gases (e.g., ammonia and amines) collaboratively initiate nucleation in urban areas (Yao et al., 2018; Shang et al., 2023), while low-volatility condensable species (e.g., sulfuric acid and oxygenated organic molecules (OOMs)) contribute to particle growth (Guo et al., 2020; Wang et al., 2020; Brean et al., 2025). However, high NO_X levels in urban air suppress OOMs formation, thereby limiting particle growth and underscoring the mechanistic complexity of anthropogenically influenced NPF (Tang et al., 2025).

Motor vehicles are a major source of urban atmospheric particles, especially primary nanoparticles (Rönkkö et al., 2017), contributing nearly half of total PNC in urban areas (Lv et al., 2023; Zhang et al., 2020; Zhang et al., 2024). Previous chamber and field studies suggested that the oxidation products of vehicle-emitted volatile organic compounds (VOCs) can significantly

https://doi.org/10.5194/egusphere-2026-6751
Preprint. Discussion started: 24 November 2026
© Author(s) 2026. CC BY 4.0 License.

promote urban nucleation and subsequent particle growth (Peng et al., 2017; Guo et al., 2020; Zhao et al., 2024; Yao et al., 2018). For instance, traffic-induced OOMs (e.g., $C_7H_{8\text{-}15}N_{0\text{-}1}O_{4\text{-}11}$) can serve as low-volatility condensable species that markedly enhance NPF (Brean et al., 2024; Brean et al., 2025; Guo et al., 2020). Notably, low-volatility condensable species in urban atmospheres do not originate solely from atmospheric oxidation, but may also be directly emitted from vehicle exhaust. Previous studies have shown that the high temperature of vehicular exhaust can facilitate the release of primary lower-volatility organic compounds and other condensable precursors in the gas phase, which, due to their low volatility, may contribute to nanoparticle growth under suitable vapor-concentration and partitioning conditions (Wu et al., 2025b; Wu et al., 2025a; Liu et al., 2024; Zhao et al., 2016, 2015). However, although vehicle-related lower-volatility organics and condensable vapors have increasingly been reported in atmospheric and source-oriented measurements (Chen et al., 2023; Okuljar et al., 2021; Olin et al., 2020), their contribution to new-particle growth under near-source traffic conditions remains difficult to quantify.

Semi-enclosed tunnel environments are dominated by vehicle emissions while photochemistry is strongly suppressed (Song et al., 2020; Song et al., 2018; Zhang et al., 2018; Zhang et al., 2020; Zhang et al., 2024), thereby providing a constrained setting for examining near-source particle growth under strong traffic influence (Brean et al., 2024; Donahue et al., 2013). Here, we conducted a two-week tunnel measurement campaign in Tianjin, China, with size-resolved PNC measurements spanning 10 nm to 10 μm, together with gaseous pollutants and meteorological parameters. This study focuses on traffic-related enhancement of new-particle growth into and within the measured 10-25 nm size range. We evaluate growth rates (GR) and formation rates (J) to compare the observed enhancement with the primary-emission reference under the adopted analytical framework (Zhang et al., 2025), and further use volatility basis set (VBS) growth modeling (Riipinen et al., 2012; Stolzenburg et al., 2018; Mohr et al., 2019) to test whether traffic-related condensable vapors could physically sustain the observed near-source growth.

https://doi.org/10.5194/egusphere-2026-6751
Preprint. Discussion started: 24 November 2026
© Author(s) 2026. CC BY 4.0 License.

2. Materials and methods

2.1 Measurements and Instruments

Tunnel measurements were conducted in the Wujinglu Tunnel (WJL Tunnel, 117°12'15'' E, 39°8'31'') from September 1 to September 14, 2023. The tunnel is located at the center of the Tianjin urban road network (Figure S6). Measurements were simultaneously performed at both the entrance and exit sites (560 meters apart), with instruments deployed inside the tunnel to measure particle number concentrations under heavy traffic influence. Under traffic-induced airflow, the entrance site (45 m inside) was used as a reference site before further accumulation of particles inside the tunnel. The tunnel features a semi-enclosed environment with an average daily traffic volume of 13,000 vehicles (56.4% gasoline and 1.7% diesel vehicles), thereby providing a traffic-dominated urban tunnel setting for this study. Moreover, Tables S5 and S6 show that the entrance site was not equivalent to open urban background air. NO_X, CO, and $PM_{2.5}$ were generally higher at the entrance than at the nearby station and further increased at the exit, supporting the use of the entrance as a less accumulated near-entrance reference for the entrance-exit comparison under selected tunnel conditions.

Particle number size distributions (PNSDs; 10 nm-10 μm) were measured with two SMPS (model 3082, TSI, USA; long DMA 3081A00) and two APS (model 3321, TSI, USA) units, operating at 3-minute and 1-minute intervals, respectively. To construct the full size distribution, data from both instruments were unified based on Stokes diameter. An effective density of 1.4 g cm^{-3} was determined and applied by matching the number concentrations in the overlap region (typically 500–700 nm). The merged size distribution was then divided into the measured 10-25 nm fraction ($PNC_{10\text{-}25}$), Aitken-mode particles (25-100 nm), accumulation-mode particles (100 nm-1 μm), and coarse-mode particles (>1 μm).

To ensure data consistency, a 6-hour collocated inter-comparison was conducted for both SMPS and APS units within the tunnel environment. A sensitivity analysis, with effective densities ranging from 1.2 to 1.8 g cm^{-3}, confirmed that the merging parameters had a negligible impact on $PNC_{10\text{-}25}$ and the reported growth-rate estimates. Additionally, a conservative instrument-based correction was applied to $PNC_{10\text{-}25}$, and measurement uncertainties were confirmed to be minor compared to the substantial $PNC_{10\text{-}25}$ enhancements observed. Detailed procedures are provided in Supporting Information S5–S7.

https://doi.org/10.5194/egusphere-2026-6751
Preprint. Discussion started: 24 November 2026
© Author(s) 2026. CC BY 4.0 License.

Relevant organic components were characterized using thermal desorption comprehensive two-dimensional gas chromatography coupled with time-of-flight mass spectrometry (TD-GC×GC-TOFMS; Hexin Instrument Co., China). These measurements provided useful constraints on the volatility range of traffic-emitted organics, but their ability to resolve very low-volatility and highly reactive species remains limited.

2.2 Data Analysis

Because the SMPS directly resolved particles only at diameters ≥10 nm, the NPF/non-NPF classification was applied operationally to particle-size evolution within the measured 10-25 nm range. Selected NPF event days exhibited sustained banana-shaped growth around midday, within the predefined 09:00-15:00 analysis window, whereas non-NPF days lacked such a feature. The same sustained pattern was observed at both the tunnel entrance and exit, enabling direct comparison of particle evolution between the two sites. Its timing and continuous size evolution, distinct from the short-lived particle bursts observed during the morning and evening rush hours, indicate that the selected NPF events were not simply driven by transient local primary emissions. Given that particles below 10 nm were not directly measured, the classification does not imply that initial nucleation was directly observed or that its location was determined. Among the four selected NPF event days during the campaign, three events (2023/09/10, 2023/09/12 and 2023/09/13) showed sufficiently continuous growth patterns and were therefore used for the quantitative analysis of GR and J_{10}, whereas one additional event was retained only for qualitative comparison.

To describe particle growth more clearly, two GR-related quantities were used in this study. First, the observed GR at the tunnel entrance and exit was estimated independently using the 50% concentration appearance time method (Lehtipalo et al., 2014; Kulmala et al., 2012). For the quantitative GR calculations, the 50% appearance-time points were determined from 10-min-averaged PNSDs, whereas the original 3-min resolution PNSDs were retained to illustrate the higher-time-resolution particle-size evolution.

$$GR_{obs}=\frac{\Delta d_p}{\Delta t}=\frac{d_2-d_1}{t_2-t_1} \quad (1)$$

where d_1 and d_2 were set to 11.24 and 25 nm, respectively, for the reported GR_{obs}, and t_1 and t_2 are their corresponding 50% appearance times. These values represent the site-specific, event-level interval-averaged apparent growth rates at the entrance and exit, respectively.

https://doi.org/10.5194/egusphere-2026-6751
Preprint. Discussion started: 24 November 2026
© Author(s) 2026. CC BY 4.0 License.

Second, the additional growth during tunnel transport was estimated from the time-aligned comparison between the entrance and exit. The exit time series was shifted backward by 6 min so that the observations at the two locations approximately represented the same air mass. Based on this comparison, a traffic-related incremental growth estimate, GR_{inc}, was calculated as

$$GR_{inc} = \frac{\Delta d_p}{\Delta t} = \frac{d_{exit,\ aligned} - d_{entrance}}{\tau} \quad (2)$$

where $d_{exit,\ aligned}$ and $d_{entrance}$ are the representative particle diameters (nm) at comparable stages after time alignment, and τ is the mean air-mass transport time in the tunnel (approximately 6 min, i.e., 360 s). GR_{inc} is used here as an estimate of the additional apparent growth during tunnel transport, rather than a directly observed GR at a single location.

Given the limited number of NPF event days, these GR-related results should be interpreted as event-constrained estimates within the measured 10-25 nm range. The event-resolved daily particle number size distributions, sink-related observations, and the GR determination procedure are provided in Figures S1-S3 and Table S1. Additional methodological details are provided in Supporting Information S7.

3. Results

3.1 Particle size distributions during NPF event and non-NPF periods

During the tunnel campaign, selected NPF event days were identified based on concurrent sustained particle-growth features within the measured 10-25 nm range at the tunnel entrance and exit, and their event-resolved daily particle number size distributions are shown in Figure S1 (Kalkavouras et al., 2020; Salma et al., 2016). The frequency of the operationally classified NPF events (28% of the total observation period) is consistent with observations in polluted regions (Wang et al., 2013; Hong et al., 2023; Zhou et al., 2021; Kalkavouras et al., 2020; Deng et al., 2020; Okuljar et al., 2021), where elevated anthropogenic precursor concentrations are known to enhance NPF and subsequent particle growth.

Figure 1a & b illustrate the particle size distributions (10-600 nm) observed throughout the tunnel campaign. During the selected NPF event days, the PNC at the tunnel exit ($4.9 \pm 2.8 \times 10^4$ cm^{-3}) was significantly higher than that at the entrance ($2.5 \pm 1.1 \times 10^4$ cm^{-3}), indicating substantial particle enhancement under strong traffic influence inside the tunnel. Furthermore, the PNC during the selected NPF event days also exceeded typical urban levels ($0.68 - 3.2 \times 10^4$ cm^{-3}) (Sowlat et

https://doi.org/10.5194/egusphere-2026-6751
Preprint. Discussion started: 24 November 2026
© Author(s) 2026. CC BY 4.0 License.

al., 2016; Vörösmarty et al., 2024; Wu et al., 2008; Zhou et al., 2020; Zhou et al., 2021; Belkacem et al., 2020; Pirjola et al., 2006), suggesting enhanced $PNC_{10\text{-}25}$ during these events.

The disparity of PNC between exit and entrance sites (ΔPNC) was approximately 1.1×10^4 cm^{-3} during non-NPF days, mainly reflecting primary vehicle exhaust and in-tunnel accumulation. In contrast, a more pronounced enhancement in ΔPNC ($1.5\text{-}4.6 \times 10^4$ cm^{-3}) was observed during the selected NPF event days. This increment occurred predominantly in the measured 10-25 nm fraction and peaked at around 10:00 am. This suggests that particles growing across the lower detection limit or continuing to grow within the measured 10-25 nm range contributed substantially to the elevated PNC during the detected new-particle growth period, beyond the primary-particle level indicated by non-NPF days (Guo et al., 2020; Chen et al., 2023; Okuljar et al., 2021; Olin et al., 2020). It should also be noted that the daytime $PNC_{10\text{-}25}$ peak did not simply follow traffic volume. During the evening rush hour of 17:00-18:00, PNC levels on NPF event and non-NPF days were comparable, indicating that traffic activity alone was insufficient to produce the event-related $PNC_{10\text{-}25}$ enhancement.

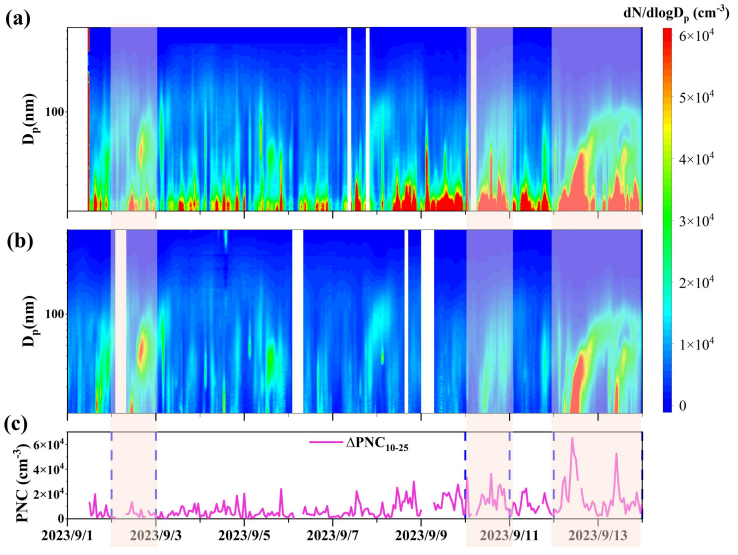

https://doi.org/10.5194/egusphere-2026-6751
Preprint. Discussion started: 24 November 2026
© Author(s) 2026. CC BY 4.0 License.

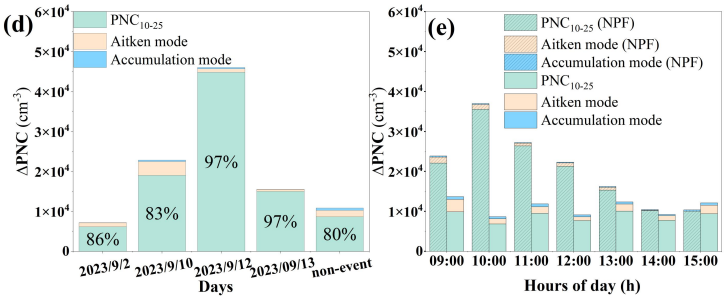

Figure 1 Particle number size distributions and new-particle growth inside the urban tunnel. Particle number size distributions from 10 nm to 0.6 μm at the tunnel exit (a) and entrance (b). Time series of $\Delta PNC_{10\text{-}25}$ (c). Contributions of the measured 10-25 nm fraction, Aitken mode, and accumulation mode to ΔPNC on individual NPF event and non-NPF days (d). Comparison of hourly average ΔPNC during NPF event and non-NPF periods from 09:00 to 15:00 (e). Selected NPF event periods are indicated by colored shading. Note: The measured 10-25 nm fraction represents the instrument-resolved portion of the conventionally defined nucleation-mode size range.

3.2 Particle growth within the tunnel environment

To estimate the NPF-event related enhancement beyond the regular entrance-exit particle increase, the average ΔPNC during non-NPF days ($1.08 \pm 0.21 \times 10^4$ cm^{-3}) was used as the primary-emission reference and subtracted from the ΔPNC on NPF event days. The derived residual size distributions are shown in Figure 2a and b. After removing this primary-emission reference, a pronounced residual entrance-exit difference remained during the selected NPF event days, especially in the measured 10-25 nm fraction (Figure 2c). This indicates that the enhanced ΔPNC during the selected NPF event days cannot be explained by the primary-emission reference alone, but reflects additional growth of particles across the lower detection limit and/or within the measured 10-25 nm range (Yao et al., 2018; Shang et al., 2023; Brean et al., 2025).

The event-mean GR_{obs} within the measured 11.24-25 nm range was higher at the exit than at the entrance (6.4 versus 5.3 nm h^{-1}; Figure 2d), with the event-specific GR determinations provided in Figure S1 and Table S1. Because GR_{obs} was derived from fixed-site observations, the higher exit value may partly reflect traffic-related enhancement of particle growth within the measured size range, possibly because particles initially below or near the detection limit grew into the detectable size range during tunnel transit. However, this entrance-exit difference alone cannot fully resolve the spatial and temporal evolution of particle growth within the tunnel. Notably, sustained growth

https://doi.org/10.5194/egusphere-2026-6751
Preprint. Discussion started: 24 November 2026
© Author(s) 2026. CC BY 4.0 License.

features became detectable earlier at the exit in all three quantitative events, with their onset at the exit preceding that at the entrance by 79 ± 36 min (Figure 2a,b). This temporal discrepancy is consistent with particles below or near the instrumental detection limit reaching ≥10 nm earlier at the exit, enabling earlier detection. Furthermore, our synchronous measurements indicated that traffic emissions were an important source of organic precursors, including S/IVOCs and heavier organics approaching C_{30} within the measured volatility window (Wu et al., 2025b; Wu et al., 2025a; Liu et al., 2024; Wu et al., 2026). While S/IVOCs are abundant in vehicle exhaust, physical constraints indicate that they are likely insufficient by themselves to sustain the observed growth (Donahue et al., 2013). In contrast, the fleet-resolved VBS estimate suggested that the lower-volatility organic vapor increment was approximately 66 ng m^{-3}, exceeding the condensed mass required to support the observed 0.7 nm growth during tunnel transit (4.9-10.1 ng m^{-3}; Section S12). Thus, the observed growth is more consistently associated with lower-volatility traffic-related condensable vapors, while the exact precursor composition cannot be uniquely resolved by the present measurements.

The particle formation rates at 10 nm (J_{10}) were also higher at the exit (10.0 cm^{-3} s^{-1}) than at the entrance (3.9 cm^{-3} s^{-1}) (Figure 2e). Notably, this enhancement occurred despite higher CS and CoagS at the exit (Figure S4a,b). Since higher CS would consume condensable vapors and higher CoagS would increase the loss of particles, the stronger $PNC_{10\text{-}25}$ enhancement at the exit cannot be attributed to more favorable sink conditions. Rather, it indicates additional particle growth into and within the measured 10-25 nm range under strong traffic influence inside the tunnel. This pattern is broadly consistent with measurements from the North China Plain (Zhou et al., 2021; Hong et al., 2023; Chu et al., 2019; Yu et al., 2017). Because our measurements were limited to particles larger than approximately 10 nm, the initial nucleation stage and subsequent sub-10 nm evolution were not directly resolved. The J_{10} values reported here therefore represent particle formation rates at 10 nm and capture only particles that survived to enter the detectable size range, rather than initial nucleation rates.

https://doi.org/10.5194/egusphere-2026-6751
Preprint. Discussion started: 24 November 2026
© Author(s) 2026. CC BY 4.0 License.

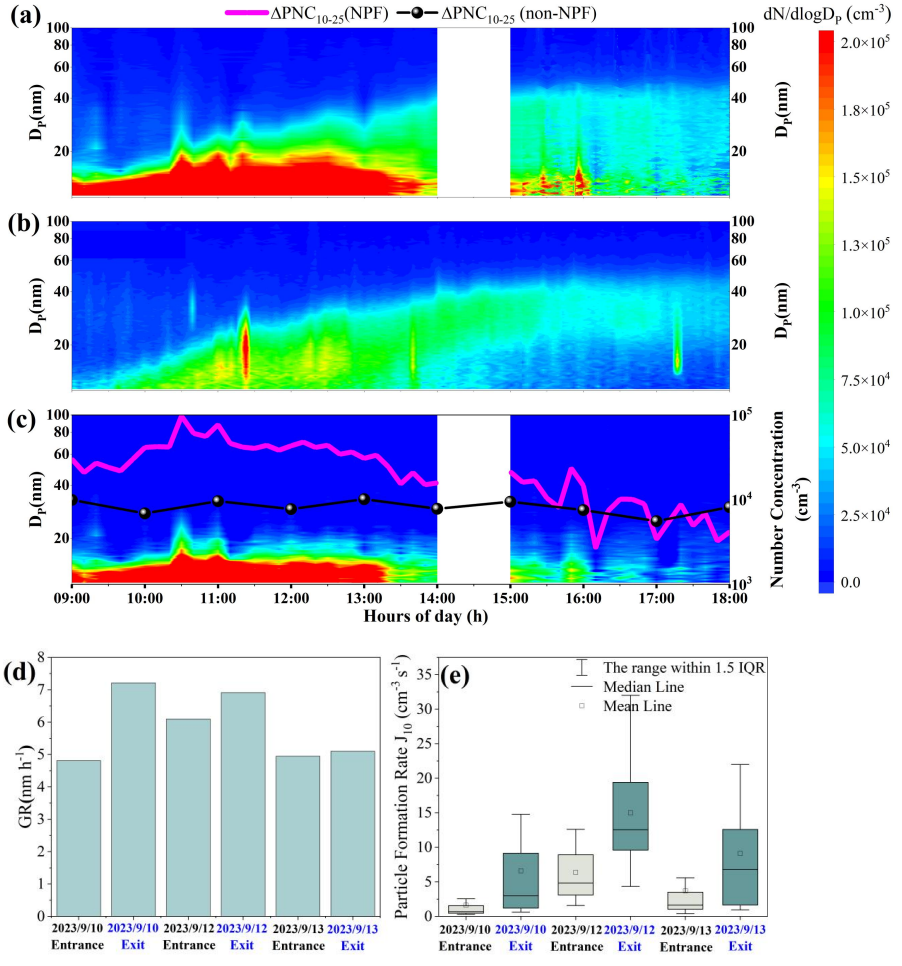

Figure 2 Particle growth dynamics during the selected NPF event days. (a) Particle size distribution at the tunnel exit; (b) comparative size distribution at the tunnel entrance; (c) size distribution of the particle number concentration difference between the exit and entrance (ΔPNC) for the representative event; (d) observed apparent growth rates; and (e) particle formation rates (J_{10}) during the continuous-growth event days. A representative event observed on September 12 is shown in panels (a)-(c). The lines in panel (c) represent $PNC_{10\text{-}25}$. The boxes in panel (e) show the interquartile range.

3.3 Traffic-related enhancement of new particle growth

Based on the size-distribution increment derived above, the traffic-related enhancement was concentrated in the measured 10-25 nm fraction ($PNC_{10\text{-}25}$) (Figure 3a). This additional $PNC_{10\text{-}25}$ contribution accounted for approximately 24.4% of the total $PNC_{10\text{-}25}$ under near-source tunnel

https://doi.org/10.5194/egusphere-2026-6751
Preprint. Discussion started: 24 November 2026
© Author(s) 2026. CC BY 4.0 License.

conditions (Figure S11), representing a conservative estimate under the adopted subtraction framework.

During the selected NPF event periods, the average PSD was well-fitted by three distinct modes, i.e., a nucleation mode near the detection limit, an Aitken mode at 61.1 nm, and an accumulation mode at 151.2 nm. In contrast, the traffic-related enhancement exhibited a single nucleation-mode peak at 11.2 nm. Traffic-related particle size distributions can vary with vehicle technology, driving conditions, and dilution processes (Ristovski et al., 2006; Gu et al., 2011; Vörösmarty et al., 2024), and previous studies have also reported fresh nanometer-scale exhaust particles (Rönkkö et al., 2017; Olin et al., 2023; Zhang et al., 2026). However, the enhancement observed during the selected NPF event periods was dominated by a narrow peak near the lower detection limit, rather than by a broader primary-exhaust particle mode. This persistent $PNC_{10\text{-}25}$ signal was mainly observed during the selected NPF event periods and remained after subtracting the primary-emission reference, supporting its interpretation as traffic-related enhancement of particle growth into or within the measured 10-25 nm range rather than a simple increase in primary exhaust particles. The sink-related analysis (Figure S4) showed differences in CS and the 11.24 nm target-particle CoagS between NPF-event and non-NPF conditions. However, the 6-min survival factor under NPF-event conditions remained close to unity, and the apparent production estimate remained positive after accounting for CoagS, indicating that coagulation loss alone cannot explain the residual enhancement in Figure 3a. Therefore, the additional near-threshold peak is consistent with an additional apparent particle-growth contribution during the selected NPF event periods. Details are provided in Supporting Information S7.

We further derived the traffic-related incremental growth estimate (GR_{inc}) and formation rates (Jinc) based on PNC. The event-mean GR_{inc}, representing the apparent growth increment over the approximately 6-min tunnel transit, was estimated to be 7.0 ± 0.9 nm h^{-1} from the three event-specific estimates reported in Table S1 (Figure 3b). Previous studies have shown that OOMs can substantially contribute to nucleation and early particle growth, especially under photochemically active conditions (Guo et al., 2020; Wang et al., 2020; Brean et al., 2024; Garmash et al., 2020; Peng et al., 2017; Donahue et al., 2013). Because sunlight was limited inside the tunnel, photochemical production of OOMs was likely suppressed. Therefore, the elevated GR_{inc} may reflect contributions from traffic-related condensable vapors emitted at or near the source. This inference is consistent

https://doi.org/10.5194/egusphere-2026-6751
Preprint. Discussion started: 24 November 2026
© Author(s) 2026. CC BY 4.0 License.

with previous studies (Donahue et al., 2011; Donahue et al., 2013; Chen et al., 2023; Kirkby et al., 2011), which also suggested that traffic-related precursor vapors can contribute to the growth of new particles under near-road conditions.

Figure 3b compares growth rates obtained across different environments and methods. GR_{inc} represents the aligned entrance-exit growth increment over the approximately 6-min tunnel transport. In contrast, the site-specific GRs reflect local apparent growth and may be affected by entrance dilution and the higher condensation sink at the exit. The derived GR_{inc} was considerably higher than values typically reported in clean regions, but fell within the range observed in polluted urban environments, suggesting rapid traffic-related nanoparticle growth under near-source conditions (Deng et al., 2020; Yu et al., 2016; Yao et al., 2018; Kontkanen et al., 2016; Boulon et al., 2010; Yu et al., 2014). In addition, the VBS growth-modeling test (Riipinen et al., 2012; Stolzenburg et al., 2018; Mohr et al., 2019; Stolzenburg et al., 2025; Stolzenburg et al., 2022) showed that fleet-emitted lower-volatility condensable vapors could produce effective GRs comparable to the observed GRinc, further supporting the physical plausibility of these vapors contributing to the observed near-source growth (Section 4.1).

Consistent with this rapid growth pattern, the analytically estimated traffic-related increment in $J_{1.5}$ (Kerminen and Kulmala, 2002; Korhonen et al., 2011) ranged from 1.3 to 104.1 cm^{-3} s^{-1} (Figure S12). These analytically derived estimates, which exceed typical rural backgrounds and align with polluted urban environments (Guo et al., 2020; Brean et al., 2024), suggest that traffic-related precursor vapors may facilitate the growth of clusters to detectable sizes under near-source tunnel conditions.

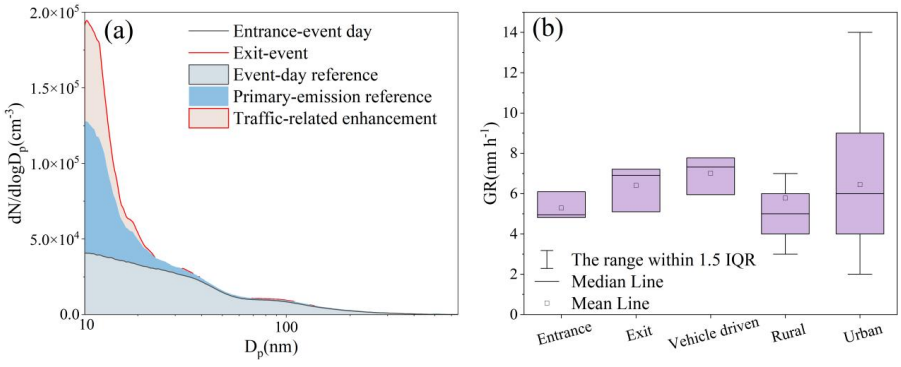

Figure 3. Traffic-related enhancement of new-particle growth in the WJL tunnel.

https://doi.org/10.5194/egusphere-2026-6751
Preprint. Discussion started: 24 November 2026
© Author(s) 2026. CC BY 4.0 License.

(a) Average particle number size distributions at the tunnel entrance and exit during the selected NPF event days, together with the NPF-event reference, primary-emission reference, and the traffic-related enhancement under the adopted subtraction framework. (b) Comparison of the observed apparent growth rates at the tunnel entrance and exit and the traffic-related incremental growth estimate with values reported in previous in-situ studies (Deng et al., 2020; Yu et al., 2016; Yao et al., 2018; Kontkanen et al., 2016; Boulon et al., 2010; Yu et al., 2014). The boxes in panel (b) show the interquartile range (IQR).

4. Discussion

The tunnel observations in this study showed clear traffic-related enhancement of nanoparticle growth during the selected NPF event days. However, because high-time-resolution measurements of low- and extremely low-volatility organic compounds (LVOCs/ELVOCs) were not available, the specific composition of the growth-relevant precursors remains uncertain. Here, we combined tunnel observations, chassis-dynamometer organic measurements, and dynamic volatility basis set (VBS) growth modeling to evaluate whether traffic-related condensable vapors could physically sustain the observed near-source particle growth.

4.1 Dynamic VBS-model constraint on traffic-related condensable vapors

To provide a physically constrained test, we used the dynamic organic growth model implemented in *aerosolpy.growth.VbsModel* (Stolzenburg et al., 2025; Stolzenburg et al., 2022), which is based on the VBS framework and has been widely applied to investigate organic-vapor-driven nanoparticle growth in chamber, field, and urban studies (Riipinen et al., 2012; Stolzenburg et al., 2018; Mohr et al., 2019). In this framework, organic compounds are grouped into discrete volatility bins, and particle growth is calculated from the transfer of vapors from the gas phase to particles. Moreover, the calculation includes gas-particle partitioning, vapor-particle collision kinetics, the Kelvin effect, and mass-transfer limitations. Model inputs were derived from chassis-dynamometer measurements of gasoline and diesel vehicle emissions, with gas- and particle-phase organics assigned to VBS bins. These emission-based volatility distributions were further constrained using tunnel traffic flow and fleet composition to estimate the contribution of different volatility classes to particle growth under tunnel conditions. Details are provided in Supporting Information S12.

The model was run under representative tunnel conditions (298.15 K, ~1 atm) with quasi-

https://doi.org/10.5194/egusphere-2026-6751
Preprint. Discussion started: 24 November 2026
© Author(s) 2026. CC BY 4.0 License.

steady organic vapor inputs over the 0-6 min transit period. To represent near-source growth during tunnel transport, simulations were initialized with 11.2 nm particles, and the predicted diameter change was converted to an effective GR for comparison with the observed GR_{inc}. Using a fleet-based estimated input of lower-volatility organic vapors ($\log_{10}C^* < 0$), corresponding to an estimated tunnel concentration increment of approximately 66 ng m^{-3}, the aerosolpy base simulation predicted an effective GR of 12.1 nm h^{-1}. Shifting the volatility distribution by ±1 VBS bin yielded predicted GRs ranging from 6.3 to 13.7 nm h^{-1}, encompassing the observed GR_{inc} (~7 nm h^{-1}). Even under a sensitivity scenario assuming strong particle-phase diffusion limitations, the predicted GR remained approximately 8.4 nm h^{-1} (Figures S13-S15). Additionally, a supplementary mass-supply check yielded a consistent result, with the condensed mass required for the observed growth estimated at 4.9-10.1 ng m^{-3}, lower than the fleet-based estimated supply of lower-volatility organic vapors. Together, these results indicate that traffic-related lower-volatility condensable organic vapors could physically sustain the observed near-source particle growth within the dynamic VBS framework.

4.2 Potential precursor pathways and study limitations

Although the dynamic VBS calculation supports the physical plausibility of traffic-related nanoparticle growth, the responsible molecular precursors cannot be uniquely identified from the present measurements. Other traffic-related precursor classes may also contribute. Previous studies have shown that OOMs can substantially contribute to nucleation and early particle growth under photochemically active conditions (Peng et al., 2017; Guo et al., 2020; Wang et al., 2020; Brean et al., 2024; Garmash et al., 2020; Donahue et al., 2013). For example, Brean et al. reported that traffic-related OOMs enhanced particle growth and survival in *Leipzig* (Brean et al., 2024). Under the low-light and low-oxidation tunnel conditions of this study, sustained photochemical OOM production was likely limited, although OOMs may still have contributed to particle growth into or within the measured size range. Moreover, roadside and polluted-urban observations have identified traffic emissions as an important source of sub-3 nm particles, and traffic-related C_2-amines can further promote particle formation (Chen et al., 2023; Brean et al., 2025). These findings indicate that multiple traffic-related condensable precursor classes may be environmentally relevant in near-source traffic microenvironments.

Therefore, the present results should not be interpreted as molecular identification of the species responsible for the observed growth, nor as evidence that a single precursor class dominated

https://doi.org/10.5194/egusphere-2026-6751
Preprint. Discussion started: 24 November 2026
© Author(s) 2026. CC BY 4.0 License.

the process. Because the SMPS measurements were limited to particles with diameters ≥10 nm, particle formation and growth below approximately 10 nm were not directly resolved. Accordingly, the present observations constrain only the entrance-exit enhancement and apparent growth within the measured 10-25 nm range and do not establish where initial nucleation occurred. The TD-GC×GC-TOFMS measurements mainly constrained relatively stable gas-phase organics within the C_6-C_{30} range, whereas key condensable vapors implicated in particle formation and growth, including LVOCs, ELVOCs, OOMs, amines, sulfuric acid, and other highly reactive species, were not comprehensively resolved, introducing additional uncertainty in identifying the responsible molecular precursors. In addition, gas-particle partitioning depends not only on volatility, but also on vapor abundance, particle loading, dilution, and subsequent chemical processing (Donahue et al., 2006; Robinson et al., 2007; Donahue et al., 2012). Thus, the observations and dynamic VBS framework provide a physically constrained indication that traffic-derived condensable vapors may contribute to near-source particle growth, while the relative importance of individual precursor classes and the persistence of this growth after atmospheric dilution remain unresolved. Future studies combining high-time-resolution precursor measurements, molecular-level characterization, dilution-aware partitioning analyses, and physically constrained modeling are needed to identify the dominant species and quantify their contributions.

5. Atmospheric implications and conclusions

This tunnel observation should be interpreted as an observational constraint on particle enhancement in a near-source traffic microenvironment, with the entrance site serving as a near-entrance reference rather than as open urban background air. Under the adopted analytical framework, traffic-related processes accounted for approximately 24.4% of the observed $PNC_{10\text{-}25}$ during the selected NPF event periods. Because the SMPS resolved particles only at diameters ≥10 nm, this estimate specifically characterizes the traffic-related contribution to sustained particle growth within the measured 10-25 nm range during tunnel transit. Moreover, the dynamic VBS calculation supports the physical plausibility of traffic-related condensable vapors contributing to this near-source growth.

When extending these results beyond the tunnel environment, the observational boundary of this study should be considered. The specific precursor species remain to be identified, as high-time-resolution measurements of LVOCs, ELVOCs, OOMs, and other condensable vapors were not

https://doi.org/10.5194/egusphere-2026-6751
Preprint. Discussion started: 24 November 2026
© Author(s) 2026. CC BY 4.0 License.

available. In addition, post-tunnel dilution, evaporation, and gas-particle repartitioning were not directly resolved, and open-road conditions may differ because of stronger dilution, more variable meteorology, and transient high-emission driving events (Brean et al., 2025; Brean et al., 2024).

Although the present findings are limited to near-source conditions, the observed enhancement in nanoparticles has important implications for traffic-related pollution assessment. This relevance is further underscored by Euro 7, which lowers the regulatory size threshold for particle-number emissions from 23 to 10 nm (Union, 2024). Previous studies have shown that nucleation-mode particles account for a substantial fraction of vehicle-emitted particle numbers (Lv et al., 2023; Straaten et al., 2023), and their respiratory deposition potential highlights their relevance to human exposure (Zhang et al., 2026). Therefore, accurately characterizing near-source changes in PNC is important for a more comprehensive assessment of traffic-related ultrafine particle pollution.

More broadly, the effects of vehicular emissions on urban particle pollution may extend beyond the direct release of particles. Previous studies have shown that vehicle-related particles can contribute to subsequent aerosol transformation through atmospheric reactions (Qi et al., 2026). Our findings suggest that, in addition to conventional regulated pollutants such as NO_X and $PM_{2.5}$, traffic-related condensable precursors associated with new-particle growth warrant further characterization in near-road and other traffic-dominated microenvironments (Tang et al., 2025). Future studies should combine detailed precursor speciation, dilution-aware measurements, volatility-resolved gas-particle partitioning analysis, sub-10 nm particle measurements, and physically constrained modeling to evaluate the atmospheric relevance of these processes across different traffic environments.

Data availability

All primary data supporting this study are available in the Supplement. As the data used in this study have not been previously published, other analyzed data of interest can be further derived from the primary data in the Supplement or obtained from the main text.

Supplement

Supplementary material associated with this article is provided in the accompanying Supporting Information file, including event-resolved particle number size distributions and growth-rate determination (Sections S1-S3); sink-related analyses and particle survival estimates (S4); measurement setup, traffic conditions, instrument calibration, and data processing methods

https://doi.org/10.5194/egusphere-2026-6751
Preprint. Discussion started: 24 November 2026
© Author(s) 2026. CC BY 4.0 License.

(S5-S7); fitted particle size-distribution modes and non-NPF-day particle number concentrations (S8-S9); source apportionment and particle formation-rate comparisons (S10-S11); dynamic VBS growth modeling and supplementary mass-supply calculations (S12); and meteorological and air-quality conditions during the tunnel campaign (S13).

Author contributions

Fuyang Zhang: Writing-original draft, Investigation, Formal analysis, Data curation, Visualization. Jinsheng Zhang: Investigation, Methodology, Data curation. Jiayuan Liu: Investigation, Data curation. Yajun Wu: Methodology, Supervision. Zongyan Lv: Methodology. Kexin Liu: Investigation, Data curation. Bin Sun: Investigation, Data curation. Qijun Zhang: Investigation, Data curation. Lin Wu: Methodology, Supervision. Miao Tang: Investigation, Project administration. Ning Yang: Resources, Data curation. Wei Hu: Investigation, Project administration. Hongjun Mao: Conceptualization, Writing-review & editing, Supervision, Funding acquisition. Jianfei Peng: Conceptualization, Methodology, Writing-review & editing, Supervision, Funding acquisition.

Competing interests

The authors declare that they have no known competing financial interests or personal relationships that could have appeared to influence the work reported in this paper.

Acknowledgments

The work was supported by the National Natural Science Foundation of China. Instrument support was provided by the Tianjin Eco-Environmental Monitoring Center and the Institute of Surface-Earth System Science, Tianjin University.

Financial support

This work was supported by the National Key Research and Development Program of China (Grant No. 2022YFE0135000), the National Natural Science Foundation of China (Grant No. 42175123, and 42405105), and the International Cooperation and Exchange of the National Natural Science Foundation of China (Grant No. 42311530112 and 42311530042).

https://doi.org/10.5194/egusphere-2026-6751
Preprint. Discussion started: 24 November 2026
© Author(s) 2026. CC BY 4.0 License.

References

Belkacem, I., Khardi, S., Helali, A., Slimi, K., and Serindat, S.: The influence of urban road traffic on nanoparticles: roadside measurements, Atmospheric Environment, 242, 117786, 2020.

Boulon, J., Sellegri, K., Venzac, H., Picard, D., Weingartner, E., Wehrle, G., Collaud Coen, M., Bütikofer, R., Flückiger, E., Baltensperger, U., and Laj, P.: New particle formation and ultrafine charged aerosol climatology at a high altitude site in the Alps (Jungfraujoch, 3580 m a.s.l., Switzerland), Atmospheric Chemistry and Physics, 10, 9333–9349, 10.5194/acp-10-9333-2010, 2010.

Brean, J., Rowell, A., Beddows, D. C., Weinhold, K., Mettke, P., Merkel, M., Tuch, T., Rissanen, M., Maso, M. D., and Kumar, A.: Road traffic emissions lead to much enhanced new particle formation through increased growth rates, Environmental Science & Technology, 58, 10664–10674, 2024.

Brean, J., Bortolussi, F., Rowell, A., Beddows, D. C. S., Weinhold, K., Mettke, P., Merkel, M., Kumar, A., Barua, S., Iyer, S., Karppinen, A., Sandström, H., Rinke, P., Wiedensohler, A., Pöhlker, M., Dal Maso, M., Rissanen, M., Shi, Z., and Harrison, R. M.: Traffic-emitted amines promote new particle formation at roadsides, ACS ES&T Air, 2, 1704–1713, 2025.

Chen, L., Qi, X., Niu, G., Li, Y., Liu, C., Lai, S., Liu, Y., Nie, W., Yan, C., and Wang, J.: High concentration of atmospheric sub-3 nm particles in polluted environment of eastern China: new particle formation and traffic emission, Journal of Geophysical Research: Atmospheres, 128, e2023JD039669, 2023.

Chu, B., Kerminen, V. M., Bianchi, F., Yan, C., Petäjä, T., and Kulmala, M.: Atmospheric new particle formation in China, Atmospheric Chemistry and Physics, 19, 115–138, 10.5194/acp-19-115-2019, 2019.

Deng, C., Fu, Y., Dada, L., Yan, C., Cai, R., Yang, D., Zhou, Y., Yin, R., Lu, Y., and Li, X.: Seasonal characteristics of new particle formation and growth in urban Beijing, Environmental Science & Technology, 54, 8547–8557, 2020.

Donahue, N., Trump, E., Pierce, J., and Riipinen, I.: Theoretical constraints on pure vapor-pressure driven condensation of organics to ultrafine particles, Geophysical Research Letters, 38, 2011.

Donahue, N. M., Kroll, J., Pandis, S. N., and Robinson, A. L.: A two-dimensional volatility basis set–Part 2: Diagnostics of organic-aerosol evolution, Atmospheric Chemistry and Physics, 12, 615–634, 2012.

Donahue, N. M., Robinson, A., Stanier, C., and Pandis, S.: Coupled partitioning, dilution, and chemical aging of semivolatile organics, Environmental Science & Technology, 40, 2635–2643, 2006.

Donahue, N. M., Ortega, I. K., Chuang, W., Riipinen, I., Riccobono, F., Schobesberger, S., Dommen, J., Baltensperger, U., Kulmala, M., and Worsnop, D. R.: How do organic vapors contribute to new-particle formation?, Faraday Discussions, 165, 91–104, 2013.

Garmash, O., Rissanen, M. P., Pullinen, I., Schmitt, S., Kausiala, O., Tillmann, R., Zhao, D., Percival, C., Bannan, T. J., Priestley, M., Hallquist, Å. M., Kleist, E., Kiendler-Scharr, A., Hallquist, M., Berndt, T., McFiggans, G., Wildt, J., Mentel, T. F., and Ehn, M.: Multi-generation OH oxidation as a source for highly oxygenated organic molecules from aromatics, Atmospheric Chemistry and Physics, 20, 515–537, 2020.

Gordon, H., Kirkby, J., Baltensperger, U., Bianchi, F., Breitenlechner, M., Curtius, J., Dias, A., Dommen, J., Donahue, N. M., and Dunne, E. M.: Causes and importance of new particle formation in the present-day and preindustrial atmospheres, Journal of Geophysical Research: Atmospheres, 122, 8739–8760, 2017.

Gu, J., Pitz, M., Schnelle-Kreis, J., Diemer, J., Reller, A., Zimmermann, R., Soentgen, J., Stoelzel, M., Wichmann, H.-E., and Peters, A.: Source apportionment of ambient particles: comparison of positive

https://doi.org/10.5194/egusphere-2026-6751
Preprint. Discussion started: 24 November 2026
© Author(s) 2026. CC BY 4.0 License.

matrix factorization analysis applied to particle size distribution and chemical composition data, Atmospheric Environment, 45, 1849–1857, 2011.

Guo, S., Hu, M., Zamora, M. L., Peng, J., Shang, D., Zheng, J., Du, Z., Wu, Z., Shao, M., and Zeng, L.: Elucidating severe urban haze formation in China, Proceedings of the National Academy of Sciences of the United States of America, 111, 17373–17378, 2014.

Guo, S., Hu, M., Peng, J., Wu, Z., Zamora, M. L., Shang, D., Du, Z., Zheng, J., Fang, X., Tang, R., Wu, Y., Zeng, L., Shuai, S., Zhang, W., Wang, Y., Ji, Y., Li, Y., Zhang, A. L., Wang, W., Zhang, F., Zhao, J., Gong, X., Wang, C., Molina, M. J., and Zhang, R.: Remarkable nucleation and growth of ultrafine particles from vehicular exhaust, Proceedings of the National Academy of Sciences of the United States of America, 117, 3427–3432, 10.1073/pnas.1916366117, 2020.

Hong, J., Tang, M., Wang, Q., Ma, N., Zhu, S., Zhang, S., Pan, X., Xie, L., Li, G., and Kuhn, U.: Measurement Report: Wintertime new particle formation in the rural area of the North China Plain–influencing factors and possible formation mechanism, Atmospheric Chemistry and Physics, 23, 5699–5713, 2023.

Kalkavouras, P., Bougiatioti, A., Grivas, G., Stavroulas, I., Kalivitis, N., Liakakou, E., Gerasopoulos, E., Pilinis, C., and Mihalopoulos, N.: On the regional aspects of new particle formation in the Eastern Mediterranean: A comparative study between a background and an urban site based on long term observations, Atmospheric Research, 239, 104911, 2020.

Kerminen, V.-M. and Kulmala, M.: Analytical formulae connecting the “real” and the “apparent” nucleation rate and the nuclei number concentration for atmospheric nucleation events, Journal of Aerosol Science, 33, 609–622, 2002.

Kirkby, J., Curtius, J., Almeida, J., Dunne, E., Duplissy, J., Ehrhart, S., Franchin, A., Gagné, S., Ickes, L., and Kürten, A.: Role of sulphuric acid, ammonia and galactic cosmic rays in atmospheric aerosol nucleation, Nature, 476, 429–433, 2011.

Kontkanen, J., Järvinen, E., Manninen, H. E., Lehtipalo, K., Kangasluoma, J., Decesari, S., Gobbi, G. P., Laaksonen, A., Petäjä, T., and Kulmala, M.: High concentrations of sub-3nm clusters and frequent new particle formation observed in the Po Valley, Italy, during the PEGASOS 2012 campaign, Atmospheric Chemistry and Physics, 16, 1919–1935, 10.5194/acp-16-1919-2016, 2016.

Korhonen, H., Sihto, S.-L., Kerminen, V.-M., and Lehtinen, K.: Evaluation of the accuracy of analysis tools for atmospheric new particle formation, Atmospheric Chemistry and Physics, 11, 3051–3066, 2011.

Kulmala, M., Petäjä, T., Nieminen, T., Sipilä, M., Manninen, H. E., Lehtipalo, K., Dal Maso, M., Aalto, P. P., Junninen, H., and Paasonen, P.: Measurement of the nucleation of atmospheric aerosol particles, Nature Protocols, 7, 1651–1667, 2012.

Lehtipalo, K., Leppä, J., Kontkanen, J., Kangasluoma, J., Franchin, A., Wimnner, D., Schobesberger, S., Junninen, H., Petäjä, T., and Sipilä, M.: Methods for determining particle size distribution and growth rates between 1 and 3 nm using the Particle Size Magnifier, Boreal Environment Research, 19, 215–236, 2014.

Lelieveld, J. and Pöschl, U.: Chemists can help to solve the air-pollution health crisis, Nature, 551, 291–293, 2017.

Li, X., Li, Y., Cai, R., Yan, C., Qiao, X., Guo, Y., Deng, C., Yin, R., Chen, Y., and Li, Y.: Insufficient condensable organic vapors lead to slow growth of new particles in an urban environment, Environmental Science & Technology, 56, 9936–9946, 2022.

https://doi.org/10.5194/egusphere-2026-6751
Preprint. Discussion started: 24 November 2026
© Author(s) 2026. CC BY 4.0 License.

Liu, P., Wu, Y., Li, Z., Lv, Z., Zhang, J., Liu, Y., Song, A., Wang, T., Wu, L., and Mao, H.: Tailpipe volatile organic compounds (VOCs) emissions from Chinese gasoline vehicles under different vehicle standards, fuel types, and driving conditions, Atmospheric Environment, 323, 120348, 2024.

Lv, Z., Peng, J., Zhang, J., Yang, L., Guo, D., Wei, N., Wu, Y., Fang, T., Song, A., Fan, C., Wu, L., Zhang, Q., and Mao, H.: Particulate emissions from gasoline vehicles using three different fuel injection technologies, Journal of Cleaner Production, 418, 10.1016/j.jclepro.2023.138123, 2023.

Mohr, C., Thornton, J. A., Heitto, A., Lopez-Hilfiker, F. D., Lutz, A., Riipinen, I., Hong, J., Donahue, N. M., Hallquist, M., and Petäjä, T.: Molecular identification of organic vapors driving atmospheric nanoparticle growth, Nature Communications, 10, 4442, 2019.

Okuljar, M., Kuuluvainen, H., Kontkanen, J., Garmash, O., Olin, M., Niemi, J. V., Timonen, H., Kangasluoma, J., Tham, Y. J., Baalbaki, R., Sipilä, M., Salo, L., Lintusaari, H., Portin, H., Teinilä, K., Aurela, M., Dal Maso, M., Rönkkö, T., Petäjä, T., and Paasonen, P.: Measurement report: The influence of traffic and new particle formation on the size distribution of 1–800 nm particles in Helsinki–a street canyon and an urban background station comparison, Atmospheric Chemistry and Physics, 21, 9931–9953, 2021.

Olin, M., Oikarinen, H., Marjanen, P., Mikkonen, S., and Karjalainen, P.: High particle number emissions determined with robust regression plume analysis (RRPA) from hundreds of vehicle chases, Environmental Science & Technology, 57, 8911–8920, 2023.

Olin, M., Kuuluvainen, H., Aurela, M., Kalliokoski, J., Kuittinen, N., Isotalo, M., Timonen, H. J., Niemi, J. V., Rönkkö, T., and Dal Maso, M.: Traffic-originated nanocluster emission exceeds H_2SO_4-driven photochemical new particle formation in an urban area, Atmospheric Chemistry and Physics, 20, 1–13, 2020.

Peng, J., Hu, M., Shang, D., Wu, Z., Du, Z., Tan, T., Wang, Y., Zhang, F., and Zhang, R.: Explosive secondary aerosol formation during severe haze in the North China Plain, Environmental Science & Technology, 55, 2189–2207, 10.1021/acs.est.0c07204, 2021.

Peng, J., Hu, M., Wang, Z., Huang, X., Kumar, P., Wu, Z., Guo, S., Yue, D., Shang, D., and Zheng, Z.: Submicron aerosols at thirteen diversified sites in China: size distribution, new particle formation and corresponding contribution to cloud condensation nuclei production, Atmospheric Chemistry and Physics, 14, 10249–10265, 2014.

Peng, J., Hu, M., Du, Z., Wang, Y., Zheng, J., Zhang, W., Yang, Y., Qin, Y., Zheng, R., Xiao, Y., Wu, Y., Lu, S., Wu, Z., Guo, S., Mao, H., and Shuai, S.: Gasoline aromatics: a critical determinant of urban secondary organic aerosol formation, Atmospheric Chemistry and Physics, 17, 10743–10752, 10.5194/acp-17-10743-2017, 2017.

Pirjola, L., Paasonen, P., Pfeiffer, D., Hussein, T., Hämeri, K., Koskentalo, T., Virtanen, A., Rönkkö, T., Keskinen, J., and Pakkanen, T.: Dispersion of particles and trace gases nearby a city highway: mobile laboratory measurements in Finland, Atmospheric Environment, 40, 867–879, 2006.

Qi, F., Liang, X., Zeng, Y., Qi, C., Liang, Z., Liu, X., Men, Z., Fang, T., Guo, J., and Ma, Y.: Unexpectedly rapid SO_2 heterogeneous reaction on the surface of vehicular brake wear particles, Nature Communications, 17, 9649, 2026.

Qi, Y., Wei, S., Xin, T., Huang, C., Pu, Y., Ma, J., Zhang, C., Liu, Y., Lynch, I., and Liu, S.: Passage of exogeneous fine particles from the lung into the brain in humans and animals, Proceedings of the National Academy of Sciences of the United States of America, 119, e2117083119, 2022.

https://doi.org/10.5194/egusphere-2026-6751
Preprint. Discussion started: 24 November 2026
© Author(s) 2026. CC BY 4.0 License.

Qiao, X., Yan, C., Li, X., Guo, Y., Yin, R., Deng, C., Li, C., Nie, W., Wang, M., and Cai, R.: Contribution of atmospheric oxygenated organic compounds to particle growth in an urban environment, Environmental Science & Technology, 55, 13646–13656, 2021.

Riipinen, I., Yli-Juuti, T., Pierce, J. R., Petäjä, T., Worsnop, D. R., Kulmala, M., and Donahue, N. M.: The contribution of organics to atmospheric nanoparticle growth, Nature Geoscience, 5, 453–458, 2012.

Ristovski, Z., Jayaratne, E., Lim, M., Ayoko, G., and Morawska, L.: Influence of diesel fuel sulfur on nanoparticle emissions from city buses, Environmental Science & Technology, 40, 1314–1320, 2006.

Robinson, A. L., Donahue, N. M., Shrivastava, M. K., Weitkamp, E. A., Sage, A. M., Grieshop, A. P., Lane, T. E., Pierce, J. R., and Pandis, S. N.: Rethinking organic aerosols: Semivolatile emissions and photochemical aging, Science, 315, 1259–1262, 2007.

Rönkkö, T., Kuuluvainen, H., Karjalainen, P., Keskinen, J., Hillamo, R., Niemi, J. V., Pirjola, L., Timonen, H. J., Saarikoski, S., and Saukko, E.: Traffic is a major source of atmospheric nanocluster aerosol, Proceedings of the National Academy of Sciences of the United States of America, 114, 7549–7554, 2017.

Salma, I., Németh, Z., Kerminen, V.-M., Aalto, P., Nieminen, T., Weidinger, T., Molnár, Á., Imre, K., and Kulmala, M.: Regional effect on urban atmospheric nucleation, Atmospheric Chemistry and Physics, 16, 8715–8728, 2016.

Shang, D., Hu, M., Tang, L., Fang, X., Chen, S., Zeng, L., Guo, S., Zhang, Y., and Wu, Z.: New particle formation occurrence in the urban atmosphere of Beijing during 2013–2020, Journal of Geophysical Research: Atmospheres, 128, e2022JD038334, 2023.

Song, C., Liu, Y., Sun, L., Zhang, Q., and Mao, H.: Emissions of volatile organic compounds (VOCs) from gasoline- and liquified natural gas (LNG)-fueled vehicles in tunnel studies, Atmospheric Environment, 234, 10.1016/j.atmosenv.2020.117626, 2020.

Song, C., Ma, C., Zhang, Y., Wang, T., Wu, L., Wang, P., Liu, Y., Li, Q., Zhang, J., Dai, Q., Zou, C., Sun, L., and Mao, H.: Heavy-duty diesel vehicles dominate vehicle emissions in a tunnel study in northern China, Science of the Total Environment, 637-638, 431–442, 10.1016/j.scitotenv.2018.04.387, 2018.

Sowlat, M. H., Hasheminassab, S., and Sioutas, C.: Source apportionment of ambient particle number concentrations in central Los Angeles using positive matrix factorization (PMF), Atmospheric Chemistry and Physics, 16, 4849–4866, 10.5194/acp-16-4849-2016, 2016.

Stolzenburg, D., Wang, M., Schervish, M., and Donahue, N. M.: Tutorial: Dynamic organic growth modeling with a volatility basis set, Journal of Aerosol Science, 166, 106063, 2022.

Stolzenburg, D., Fischer, L., Vogel, A. L., Heinritzi, M., Schervish, M., Simon, M., Wagner, A. C., Dada, L., Ahonen, L. R., and Amorim, A.: Rapid growth of organic aerosol nanoparticles over a wide tropospheric temperature range, Proceedings of the National Academy of Sciences of the United States of America, 115, 9122–9127, 2018.

Stolzenburg, D., Sarnela, N., Bianchi, F., Cai, J., Cai, R., Cheng, Y., Dada, L., Donahue, N. M., Grothe, H., and Holm, S.: Incomplete mass closure in atmospheric nanoparticle growth, npj Climate and Atmospheric Science, 8, 75, 2025.

Straaten, A., Nguyen, M.-H., and Weber, S.: Real world ultrafine particle emission factors for road-traffic derived from multi-year urban flux measurements using eddy covariance, Environmental Science: Atmospheres, 3, 1439–1452, 2023.

Tang, L., Feng, Z., Shang, D., Zeng, L., Wu, Z., Wang, H., Chen, S., Li, X., Zeng, L., Hu, J., and Hu, M.: Ongoing uncoordinated anthropogenic emission abatement promotes atmospheric new particle growth in a Chinese megacity, Nature Communications, 16, 6720, 10.1038/s41467-025-62011-6, 2025.

https://doi.org/10.5194/egusphere-2026-6751
Preprint. Discussion started: 24 November 2026
© Author(s) 2026. CC BY 4.0 License.

Union, E.: Regulation (EU) 2024/1257 of the European Parliament and of the Council of 24 April 2024 on Type-Approval of Motor Vehicles and Engines and of Systems, Components and Separate Technical Units Intended for Such Vehicles, with Respect to Their Emissions and Battery Durability (Euro 7), Amending Regulation (EU) 2018/858 of the European Parliament and of the Council and Repealing Regulations (EC) No 715/2007 and (EC) No 595/2009 of the European Parliament and of the Council, Commission Regulation (EU) No 582/2011, Commission Regulation (EU) 2017/1151, Commission Regulation (EU) 2017/2400 and Commission Implementing Regulation (EU) 2022/1362, Off. J. Eur. Union, 50, 1–49, 2024.

Vörösmarty, M., Hopke, P. K., and Salma, I.: Attribution of aerosol particle number size distributions to main sources using an 11-year urban dataset, Atmospheric Chemistry and Physics, 24, 5695–5712, 10.5194/acp-24-5695-2024, 2024.

Wang, M., Chen, D., Xiao, M., Ye, Q., Stolzenburg, D., Hofbauer, V., Ye, P., Vogel, A. L., Mauldin III, R. L., and Amorim, A.: Photo-oxidation of aromatic hydrocarbons produces low-volatility organic compounds, Environmental Science & Technology, 54, 7911–7921, 2020.

Wang, Z., Hu, M., Sun, J., Wu, Z., Yue, D., Shen, X., Zhang, Y., Pei, X., Cheng, Y., and Wiedensohler, A.: Characteristics of regional new particle formation in urban and regional background environments in the North China Plain, Atmospheric Chemistry and Physics, 13, 12495–12506, 2013.

Wu, Y., Liu, P., Wang, Y., Wang, X., Zhang, J., Liu, Y., Zhang, J., Wu, L., Wang, T., and Mao, H.: Intermediate and semi-volatility organic compounds (I/SVOCs) emission from Chinese vehicles: volatility distribution, influencing factors, and implication for SOA formation, Frontiers of Environmental Science & Engineering, 19, 70, 2025a.

Wu, Y., Zhong, C., Zhang, T., Sun, J., Liu, Y., Zhang, J., Song, P., Liu, D., Wu, L., Wang, T., Mao, H., and Peng, J.: Process-specific evaporative emission of semivolatile/intermediate-volatility organic compounds from modern gasoline vehicles, Environmental Science & Technology, 60, 8039–8050, 2026.

Wu, Y., Peng, J., Wang, X., Liu, P., Liu, Y., Zhang, F., Zhang, J., Sun, B., Zhang, J., Song, K., Song, P., Wu, L., Wang, T., Guo, S., and Mao, H.: Emissions and potential tracer screening of semivolatile/intermediate-volatility organic compounds from urban vehicle fleets, npj Climate and Atmospheric Science, 8, 186, 2025b.

Wu, Z., Hu, M., Lin, P., Liu, S., Wehner, B., and Wiedensohler, A.: Particle number size distribution in the urban atmosphere of Beijing, China, Atmospheric Environment, 42, 7967–7980, 2008.

Yao, L., Garmash, O., Bianchi, F., Zheng, J., Yan, C., Kontkanen, J., Junninen, H., Mazon, S. B., Ehn, M., and Paasonen, P.: Atmospheric new particle formation from sulfuric acid and amines in a Chinese megacity, Science, 361, 278–281, 2018.

Yu, H., Ren, L., and Kanawade, V. P.: New particle formation and growth mechanisms in highly polluted environments, Current Pollution Reports, 3, 245–253, 2017.

Yu, H., Zhou, L., Dai, L., Shen, W., Dai, W., Zheng, J., Ma, Y., and Chen, M.: Nucleation and growth of sub-3 nm particles in the polluted urban atmosphere of a megacity in China, Atmospheric Chemistry and Physics, 16, 2641–2657, 10.5194/acp-16-2641-2016, 2016.

Yu, H., Ortega, J., Smith, J. N., Guenther, A. B., Kanawade, V., You, Y., Liu, Y., Hosman, K., Karl, T., and Seco, R.: New particle formation and growth in an isoprene-dominated Ozark forest: From sub-5 nm to CCN-active sizes, Aerosol Science and Technology, 48, 1285–1298, 2014.

Zhang, F., Peng, J., Zhang, J., Liu, J., Wu, Y., Liu, P., Liu, K., Sun, B., Zhang, Q., Wu, L., Yang, N., Hu, W., and Mao, H.: Real world particle size distribution from vehicle fleet and implication on emission control, npj Clean Air, 1, 8, 10.1038/s44407-025-00007-8, 2025.

https://doi.org/10.5194/egusphere-2026-6751
Preprint. Discussion started: 24 November 2026
© Author(s) 2026. CC BY 4.0 License.



678 Zhang, F., Peng, J., Liu, P., Wu, Y., Zhang, J., Liu, J., Liu, K., Sun, B., Zhang, Q., Wu, L., Yang, N., Tang,
679 M., Hu, W., and Mao, H.: Unregulated delayed emissions dominate ultrafine particles from modern diesel
680 vehicles, Journal of Hazardous Materials, 514, 142801, 2026.
681 Zhang, J., Peng, J., Song, A., Du, Z., Guo, J., Liu, Y., Yang, Y., Wu, L., Wang, T., Song, K., Guo, S.,
682 Collins, D., and Mao, H.: Secondary organic aerosol formation potential from vehicular non-tailpipe
683 emissions under real-world driving conditions, Environmental Science & Technology, 58, 5419–5429,
684 10.1021/acs.est.3c06475, 2024.
685 Zhang, J., Peng, J., Song, C., Ma, C., Men, Z., Wu, J., Wu, L., Wang, T., Zhang, X., Tao, S., Gao, S.,
686 Hopke, P. K., and Mao, H.: Vehicular non-exhaust particulate emissions in Chinese megacities: Source
687 profiles, real-world emission factors, and inventories, Environmental Pollution, 266, 115268,
688 10.1016/j.envpol.2020.115268, 2020.
689 Zhang, Q., Wu, L., Fang, X., Liu, M., Zhang, J., Shao, M., Lu, S., and Mao, H.: Emission factors of
690 volatile organic compounds (VOCs) based on the detailed vehicle classification in a tunnel study, Science
691 of the Total Environment, 624, 878–886, 10.1016/j.scitotenv.2017.12.171, 2018.
692 Zhang, R., Khalizov, A., Wang, L., Hu, M., and Xu, W.: Nucleation and growth of nanoparticles in the
693 atmosphere, Chemical Reviews, 112, 1957–2011, 2012.
694 Zhao, B., Donahue, N. M., Zhang, K., Mao, L., Shrivastava, M., Ma, P.-L., Shen, J., Wang, S., Sun, J.,
695 and Gordon, H.: Global variability in atmospheric new particle formation mechanisms, Nature, 631, 98–
696 105, 2024.
697 Zhao, Y., Nguyen, N. T., Presto, A. A., Hennigan, C. J., May, A. A., and Robinson, A. L.: Intermediate
698 volatility organic compound emissions from on-road diesel vehicles: chemical composition, emission
699 factors, and estimated secondary organic aerosol production, Environmental Science & Technology, 49,
700 11516–11526, 2015.
701 Zhao, Y., Nguyen, N. T., Presto, A. A., Hennigan, C. J., May, A. A., and Robinson, A. L.: Intermediate
702 volatility organic compound emissions from on-road gasoline vehicles and small off-road gasoline
703 engines, Environmental Science & Technology, 50, 4554–4563, 2016.
704 Zheng, H., Wu, D., Wang, S., Li, X., Jin, L. N., Zhao, B., Li, S., Sun, Y., Dong, Z., and Wu, Q.: Control
705 of toxicity of fine particulate matter emissions in China, Nature, 643, 404–411, 2025.
706 Zhou, Y., Dada, L., Liu, Y., Fu, Y., Kangasluoma, J., Chan, T., Yan, C., Chu, B., Daellenbach, K. R., and
707 Bianchi, F.: Variation of size-segregated particle number concentrations in wintertime Beijing,
708 Atmospheric Chemistry and Physics, 20, 1201–1216, 2020.
709 Zhou, Y., Hakala, S., Yan, C., Gao, Y., Yao, X., Chu, B., Chan, T., Kangasluoma, J., Gani, S., and
710 Kontkanen, J.: Measurement report: New particle formation characteristics at an urban and a mountain
711 station in northern China, Atmospheric Chemistry and Physics, 21, 17885–17906, 2021.